Biomedicine & Pharmacotherapy 161 (2023) 114512

Contents lists available at ScienceDirect

Biomedicine & Pharmacotherapy

journal homepage: www.elsevier.com/locate/biopha

# Targeting oncogenic functions of *miR-301a* in head and neck squamous cell carcinoma by PI3K/PTEN and MEK/ERK pathways

Rocío Granda-Díaz [a,b,c,1], Lorea Manterola [d,1], Francisco Hermida-Prado [a,b,c], René Rodríguez [c,e,f], Laura Santos [a,b], Vanessa García-de-la-Fuente [a,b], María Teresa Fernández [g], M. Daniela Corte-Torres [h], Juan P. Rodrigo [a,b,c], Saúl Álvarez-Teijeiro [a,b,c,*], Charles H. Lawrie [d,i,j,k,**], Juana M. Garcia-Pedrero [a,b,c,*]

[a] *Instituto Universitario de Oncología del Principado de Asturias (IUOPA), University of Oviedo, Oviedo, Spain*
[b] *Department of Otolaryngology, Hospital Universitario Central de Asturias and Instituto de Investigación Sanitaria del Principado de Asturias (ISPA), University of Oviedo, Oviedo, Spain*
[c] *CIBERONC, Instituto de Salud Carlos III, Madrid, Spain*
[d] *Molecular Oncology group, Biodonostia Research Institute, San Sebastián, Spain*
[e] *Instituto Universitario de Oncología del Principado de Asturias (IUOPA), University of Oviedo, Oviedo, Spain*
[f] *Sarcomas and Experimental Therapies, Instituto de Investigación Sanitaria del Principado de Asturias (ISPA), University of Oviedo, Oviedo, Spain*
[g] *Histopathology Unit, Instituto Universitario de Oncología del Principado de Asturias (IUOPA), University of Oviedo, Oviedo, Spain*
[h] *Biobank of Principado de Asturias, Instituto de Investigación Sanitaria del Principado de Asturias (ISPA), Oviedo, Spain*
[i] *IKERBASQUE, Basque Foundation for Science, Bilbao, Spain*
[j] *Radcliffe Department of Medicine, University of Oxford, Oxford, United Kingdom*
[k] *Sino-Swiss Institute of Advanced Technology (SSIAT), Shanghai University, Shanghai, China*

ARTICLE INFO

*Keywords:*
Head and neck squamous cell carcinoma
*miR-301a*
Therapeutic target
Signaling
PI3K
ERK

ABSTRACT

Treatment of head and neck squamous cell carcinomas (HNSCC), the sixth most frequent cancer worldwide, remains challenging. miRNA dysregulation is closely linked to tumorigenesis and tumor progression, thus emerging as suitable targets for cancer treatment. Transcriptomic analysis of TCGA HNSCC dataset revealed that *miR-301a* expression levels significantly increased in primary tumors, as compared to patient-matched normal tissue. This prompted us to investigate its pathobiological role and potential as new therapeutic target using different preclinical HNSCC models. *miR-301a* overexpression in HNSCC-derived cell lines led to enhanced proliferation and invasion, whereas *miR-301* inhibition reduced these effects. *In vivo* validation was performed using an orthotopic mouse model. Results concordantly showed that the mitotic counts, the percentage of infiltration depth and Ki67 proliferative index were significantly augmented in the subgroup of mice harboring *miR*-301a-overexpressing tumors. Further mechanistic characterization revealed PI3K/PTEN/AKT and MEK/ERK pathways as central signaling nodes responsible for mediating the oncogenic activity of *miR-301a* observed in HNSCC cells. Notably, pharmacological disruption of PI3K and ERK signals with BYL-719 and PD98059, respectively, was effective to completely revert/abolish *miR-301a*-promoted tumor cell growth and invasion. Altogether, these findings demonstrate that *miR-301a* dysregulation plays an oncogenic role in HNSCC, thus emerging as a candidate therapeutic target for this disease. Importantly, available PI3K and ERK inhibitors emerge as promising anti-tumor agents to effectively target *miR-301a*-mediated signal circuit hampering growth-promoting and pro-invasive functions.

*Abbreviations:* ATCC, American Type Culture Collection; BSA, Bovine Serum Albumin; DMSO, Dimethyl sulfoxide; HNSCC, head and neck squamous cell carcinomas; miRNAs, MicroRNAs; TCGA, The Cancer Genome Atlas; UALCAN, The University of Alabama at Birmingham CANcer data analysis Portal.

* Correspondence to: Instituto de Investigación Sanitaria del Principado de Asturias (ISPA), Oviedo, Spain.
** Correspondence to: Biodonostia Research Institute, San Sebastián, Spain.
*E-mail addresses:* saul.teijeiro@gmail.com (S. Álvarez-Teijeiro), charles.lawrie@biodonostia.org (C.H. Lawrie), juanagp.finba@gmail.com (J.M. Garcia-Pedrero).
[1] These authors contributed equally to this work.

https://doi.org/10.1016/j.biopha.2023.114512
Received 27 January 2023; Received in revised form 7 March 2023; Accepted 9 March 2023
Available online 16 March 2023

## 1. Background

Head and neck squamous cell carcinomas (HNSCC) have a high prevalence worldwide, with 900,000 new cases per year, causing approximately 500,000 deaths [1,2]. Elevated mortality rates are related to late diagnosis, limited treatment options and tumor recurrence, highlighting an urgent need to develop novel molecular-targeted therapies for personalized medicine [3].

microRNAs (miRNAs) are non-coding single-stranded RNA of approximately 22 nucleotides in length that play an important role in post-transcriptional gene expression regulation [4]. Altered expression levels of miRNAs has been increasingly reported in a wide range of cancers, and also found to be actively involved in tumor progression and metastatic dissemination. On this basis, several works have shown that the inhibition of the seed region of these molecules could alter tumor progression, suggesting their potential use as therapeutic targets [5–7].

The *miR-130* gene family is composed by four miRNA precursors: mir-301a (located at chromosome 17), mir-130a (chromosome 11), mir-130b and mir-301b (both located at chromosome 22). *miR-130* family members are considered an oncogenic superfamily due to their capability to target tumor suppressor genes, such as *SMAD4, PTEN* or *WNT1* [8–10]. It has been demonstrated that *miR-130b*, *miR-301a* and *miR-301b* promote in vitro tumor invasion and migration in bladder cancer through FAK and AKT signaling, by regulating PTEN, postulating these miRNAs as promising therapeutic targets for this disease [9]. Accumulating evidence indicates that aberrant expression of *miR-301a* (i.e., hsa-*miR-301a*-3p) might be implicated in several important biological and pathological processes, including inflammation, oxidative stress and apoptosis [11–13]. Importantly, increased levels of *miR-301a* have been correlated with pro-metastatic phenotypes, tumor relapse and poor prognosis in patients with breast cancer, malignant melanoma, prostatic cancer and gastric carcinoma [14–20]. Moreover, *miR-301a* inhibition diminished metastases through *RUNX3* regulation, and enhanced the recruitment of immune components in a lung cancer murine model [21].

Nevertheless, the pathobiological role of this miRNA has been scarcely studied in HNSCC. This prompted us to investigate the expression status and oncogenic role of *miR-301a* in HNSCC, thereby uncovering valuable functional and mechanistic insights supporting its potential application as a therapeutic target for this disease, and unprecedentedly demonstrating PI3K and ERK pathways as central signalling nodes to interfere *miR-301a*-mediated protumorigenic functions.

## 2. Methods

### 2.1. Cell lines and culture conditions

HNSCC cell lines (larynx) UT-SCC8, UT-SCC29, UT-SCC38, UT-SCC42A, and UT-SCC42B were kindly provided by Dr. Reidar Grenman (Department of Otolaryngology, University Central Hospital, Turku, Finland) [22]. FaDu cells (pharynx) were purchased from ATCC (Manassas, Virginia, USA).

All cell lines were grown in DMEM media (Corning 10–017-CV, NY, USA) supplemented with 10% fetal bovine serum (Corning Media Tech 35–079-CV, NY, USA), 100 U/mL penicillin (Biowest, Nuaille, France), 200 mg/mL streptomycin (Biowest, Nuaille, France), 2 mM L-glutamine, 20 mM HEPES (pH 7.3) (Biowest, Nuaille, France) and 100 mM MEM non-essential amino acids (Biowest, Nuaille, France).

### 2.2. Drugs

BYL-719 (Selleckchem, Houston, TX) and PD98059 (MedChemExpress, NJ, USA) were prepared as 10 mM solutions in sterile DMSO, aliquoted and stored at − 80 °C until use to treat HNSCC cells, when they were brought to the desired final concentration. DMSO was used as the vehicle control condition.

### 2.3. Lentivirus transduction

Lentiviral transductions were performed as previously described [23,24]. In brief, cells were transduced with lentiviruses containing either *miR-301a* (InteRNA technologies) or an inhibitor (lenti miRNA inhb hum *hsa-miR-301a-3p*, ref HLTUD044, Sigma, St Louis, MO, USA) at a MOI of 1 before selection in the presence of 1 μg/mL puromycin (Sigma, La Jolla CA, USA) for 3 days and then maintained at 0.1 μg/mL puromycin.

### 2.4. RNA extraction and RT-qPCR analysis

Total RNA was extracted from cell lines using Trizol as described by the manufacturer (Life Technologies, Paisley, UK). *miR-301a-3p* was analyzed using Taqman individual miRNA assays (assay ID: 000528, Applied Biosystems) following the manufacturer's instructions. U48 was used as control gene (assay ID: 001006), as previously described [25]. Reactions were carried out in triplicate on an Applied Biosystems 7900HT PCR System. The mean Ct value of each triplicate was used for analysis. The ΔCt method (ΔCt = mean Ct of U48 – mean Ct of miR-301a) was applied for HNSCC cell lines expression analysis, and $2^{-\Delta\Delta Ct}$ method for lentiviral transduced expression analysis.

### 2.5. Cell viability assay

HNSCC cell lines were seeded into 96-well tissue culture plates at a density of 1500 – 2000 cells *per* well. After overnight incubation cell viability, in quadruplicate, by MTS assay (CellTiter 96 Aqueous One Solution Cell Proliferation Assay from Promega, Madison, WI, USA) carried out according to the manufacturer's protocol. The resulting absorbance at 490 nm was measured using a Synergy HT plate reader (BioTek, Winooski, VT, USA).

### 2.6. Colony formation assay

HNSCC cell lines were seeded at a low confluence (3000–5000 cells) in 12-well culture plates. An MTS assay was performed in order to verify that the same number of cells were initially plated in each condition. After 9–12 days, cells were fixed with methanol at room temperature, and stained with crystal violet (0.1% w/v). Where indicated treatment was renewed every two days. Afterwards, colony formation was analyzed using a GelCount scanner (Oxford Optronix Ltd) and quantified by Image J analysis software. Data were normalized to the scramble control condition.

### 2.7. Three-dimensional spheroid invasion assay

Invasion assays using 3D tumor spheroids were performed as previously described [26]. In brief, cells were suspended in DMEM plus 5% Methyl cellulose (Sigma, St Louis, MO, USA) at 80,000 cells/mL by serial pipetting into a non-adhesive Petri dish (2000 cells/spheroid), After 24 h incubation spheroids were individually transferred into a 96-well culture plate and embedded with bovine collagen matrix (Advanced Biomatrix PureCol) with an overlay of complete media. After drug treatment, cell invasion was monitored using a Zeiss Cell Observer Live Imaging microscope (Zeiss, Thornwood, NY, USA) with images taken every 15 min for 24 h. The invasive area was calculated as the difference between the final area (t = 24 h) and the initial area (t = 0 h) using image J analysis program, and data were normalized to control condition (either scramble or vehicle-treated cells, as indicated). At least three independent experiments were performed in quadruplicate for each condition tested.

### 2.8. Phosphoproteome array

Total protein was extracted from UT-SCC38 cells transduced with

*miR-301a*, *miR-301a* inhibitor and scramble control using lysis buffer (R&D Systems, Minneapolis, MN). 600 μg of each cell lysate was applied to the Proteome Profiler Human Phospho-Kinase Array Kit from R&D Systems in accordance with the manufacturer's instructions (ARY003C; R&D Systems, Minneapolis, MN). Membranes were scanned with Odyssey Fc Dual-Mode Imaging System (LI-COR Biosciences), and signal density analysis was performed using Image Studio Lite software (LI-COR Biosciences). Based on the output data, a heatmap was built using Morpheus software (https://software.broadinstitute.org/morpheus). Individual validation of specific phosphorylated proteins was carried out by Western blot analysis.

### 2.9. Western blot analysis

Cells cultures at approximately 80% confluence were lysed in Laemmli sample buffer and sonicated before centrifugation and protein concentration measured by Pierce BCA protein assay kit (Thermo Fisher, Rockford, IL). Subsequently protein lysates were loaded onto 9–12% SDS–polyacrylamide gel electrophoresis (SDS–PAGE) gels be and transferred to nitrocellulose membranes (Amersham Protran, GE Healthcare, Pittsburg, PA, USA). Membranes were blocked with 5% bovine serum albumin (BSA) for 1 h before incubating with either phospho- P44/42 MAPK (Erk 1/2) (Cell Signaling # 4370), Erk 1/2 (Cell Signaling # 9102), PTEN (Cell Signaling # 9552), phospho-Akt (T308) (Cell Signaling # 4056), Akt (Cell Signaling # 9272), phospho-Akt (S473) (Cell Signaling # 9271), phospho-S6 (S240/244) (Cell Signaling #5364), S6 Ribosomal Protein (5G10) (Cell Signaling # 2217) and β-actin (dilution 1:10,000 for 1 h; Sigma Aldrich #AC15) antibodies in a 1 in 1000 dilution. Secondary antibodies anti-rabbit and anti-mouse IRDye 800CW and IRDye 680RD (LI-COR Biosciences) were used at 1:10000 dilution for detection. The membranes were scanned using an Odyssey Fc Dual-Mode Imaging System (LI-COR Biosciences) using the red (700 nm) and green (800 nm) channels, and signal analysis was performed using Image Studio Lite software (LI-COR, Nebraska). Results were normalized to β-actin as loading control.

### 2.10. In vivo orthotopic HNSCC model

Female athymic 6-week old NMRI-nude mice of (Envigo) were inoculated sublingually with 300,000 UT-SCC38 cells in three groups (scramble, *miR-301a* and *miR-301*a inhibitor, n = 7 in each group). After 17 days, all mice were euthanized. Tissue sampling post-mortem was conducted by surgically removing the mandible and tongue from each animal. After decalcification, tissue samples were embedded in paraffin, cut into 3–4 μm slides, stained with hematoxylin and eosin (H&E), and examined histopathologically. The tumor infiltration depth (infiltration depth and extent of epithelial disruption in the tongue),mitotic count rates (total number of mitotic cells counted in three microscope fields at 40x magnification), and proliferative index (by Ki67-positive immunostaining) were evaluated by a pathologist. All experimental protocols were performed in accordance with the institutional guidelines of the University of Oviedo and approved by the Animal Research Ethical Committee of the University of Oviedo prior to the study (date of approval 2 September 2015; approval number PROAE46/2015).

Ki67 immunostaining was performed in an automatic workstation (Dako Autostainer Plus) with anti-Ki67 (Clone MIB-1 Dako # JR626, Prediluted), using the Dako EnVision Flex + Visualization System (Dako Autostainer). Quantification of Ki67 proliferation index was calculated as the percentage Ki67-positive nuclei counted at 40x in four independent microscopic fields per tissue section, and the mean for each mice group was calculated.

### 2.11. In silico analysis using transcriptomic data from the cancer genome atlas (TCGA) HNSCC database

Expression levels of *miR-301a* from RNAseq data of 482 HNSCC samples and 44 healthy tissue samples retrieved from The Cancer Genome Atlas (TCGA) (TCGA-Firehose Legacy dataset) using the online webtool UALCAN (http://ualcan.path.uab.edu/, access date 25 July 2022) [27].

### 2.12. Statistical analysis

Statistical analysis was performed using GraphPad Prism software version 8.0 (Graphpad Software Inc, La Jolla, CA, USA). Data are represented as the mean ± standard deviation (SD) of at least three independent experiments unless otherwise stated. The student's unpaired t-test with two-tailed distribution was employed for comparison across two groups, whereas one/two-way ANOVA was used for comparisons among multiple samples/variables. Significance was set at $p < 0.05$ (* $p < 0.05$; ** $p < 0.01$; *** $p < 0.001$; **** $p < 0.0001$).

## 3. Results

### 3.1. Up-regulation of miR-301a expression is commonly detected in HNSCC patient samples

*miR-301a* expression levels were assessed using transcriptomic data from a TCGA cohort of 530 HNSCC patients [28] using UALCAN online resources (http://ualcan.path.uab.edu/) [27]. As shown in Fig. 1, *miR-301a* was among the top 10 most upregulated miRNAs in the TCGA HNSCC dataset (Fig. 1 **A**). *miR-301a* expression levels significantly increased in primary tumors (n = 482) as compared to patient-matched normal tissue (n = 44) ($p < 0.0001$) (Fig. 1**B**). Concordantly, the levels of all *miR-130* family members were also found to significantly increase in primary HNSCC samples ($p < 0.0001$) (Fig. 1**C-E**).

### 3.2. Pathobiological role of miR-301a upregulation in HNSCC

We next investigated the pathobiological role and functional consequences of *miR-301a* dysregulation in HNSCC preclinical models. First, *miR-301a* levels were analyzed by qRT-PCR in a panel of six HNSCC-derived cell lines (Fig. 2**A**). UT-SCC38, UT-SCC42B, and FaDu cell lines were selected to evaluate the functional impact of lentiviral overexpression and inhibition of *miR-301a* expression. As shown in Fig. 2**B,** all three cell lines stably transduced with *miR-301a*-expressing lentivirus exhibited at least a 10-fold increase in the levels of this miRNA. Moreover, stable *miR*-301a inhibitor expression led to a 2-fold reduction of endogenous *miR-301a* levels in both UT-SCC42B and UT-SCC38 cells, whereas a smaller effect was observed in FaDu cells that displayed lower basal *miR-301a* expression.

We performed colony formation assay to evaluate the phenotypic effects of *miR-301a* expression modulation on cell proliferation. We observed that *miR-301a* over-expression significantly increased the proliferation of UT-SCC38 and FaDu cells; however, it had no effect on UT-SCC42B cells (Fig. 3). Concordantly, *miR-301a* expression inhibition significantly decreased proliferation in both UT-SCC38 and FaDu cells, whereas no noticeable effect was observed in UT-SCC42B cells. We next investigated the role of *miR-301a* in tumor invasion using a 3D spheroid invasion assay. Overexpression of *miR-301a* significantly increased UT-SCC38 cells 3D invasion, whereas *miR-301a* inhibition abrogated this effect (Fig. 4 and Supplementary Videos S1-S3). Analogous experiments were carried out in both UT-SCC42B and FaDu cells; however, no differences in spheroid invasion were observed (Supplementary Fig. S1 and S2). In parallel to these invasion assays, we performed MTS analysis at 24 h to rule out any potential proliferative effects of *miR-301a*. As shown in Supplementary Fig. S3, no significant changes on cell viability were observed at 24 h. Accordingly, we can conclude from these results that the potent effects in UT-SCC38 are truly due to cell invasion not growth.

Supplementary material related to this article can be found online at doi:10.1016/j.biopha.2023.114512.

Supplementary material related to this article can be found online at

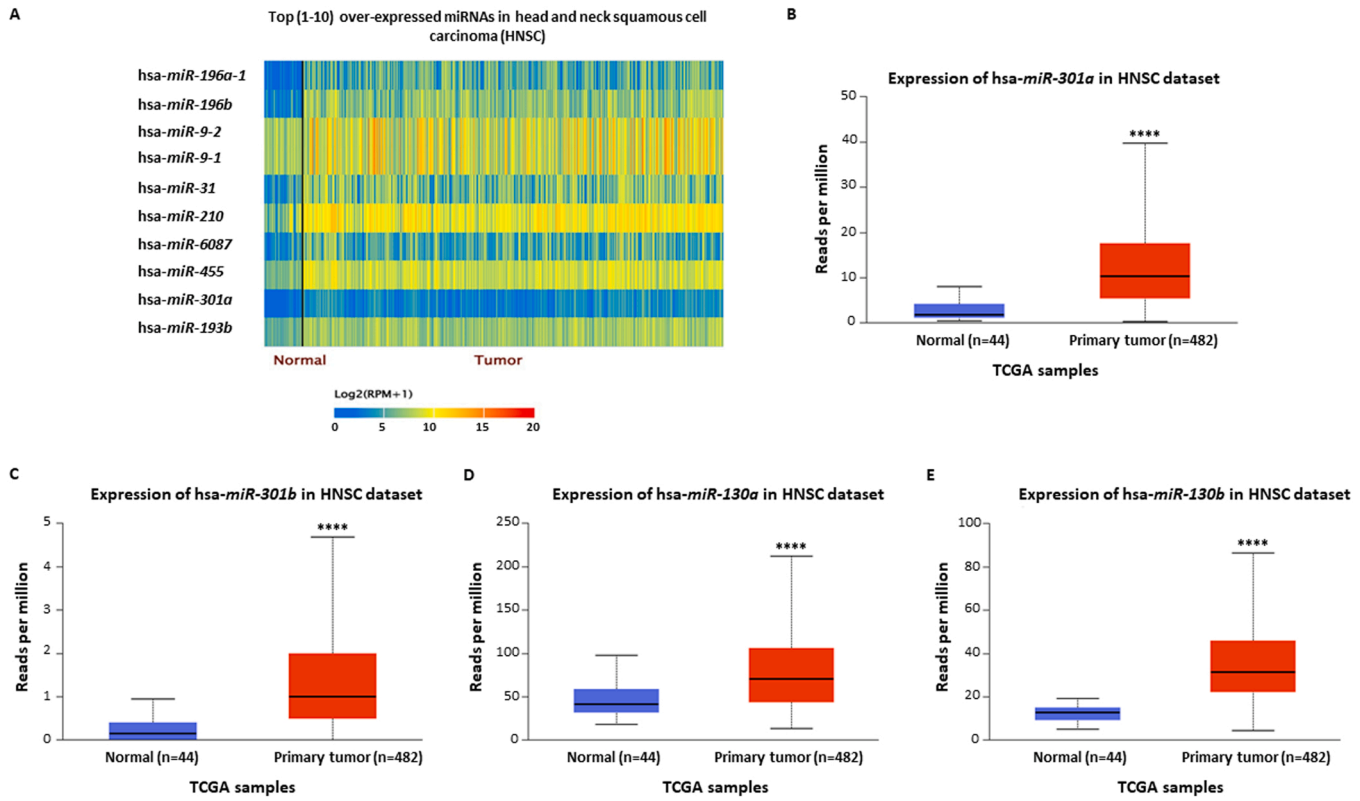


**Fig. 1.** In silico *miR-130* family expression analysis in the TCGA HNSCC dataset. *In silico* analysis was performed using RNA-seq data from a TCGA cohort of 530 HNSCC patients by UALCAN webtools (http://ualcan.path.uab.edu/) [27]. **A)** Heatmap shows the top 10 highest overexpressed miRNAs. Box plots illustrate comparisons of *miR*NA expression levels in primary tumors (n = 482) versus patient-matched normal tissue (n = 44) for **B)** *miR-301a* expression; **C)** *miR-301b* expression; **D)** *miR-130a expression*; and **E)** *miR-130b* expression. * ** * $p < 0.0001$.

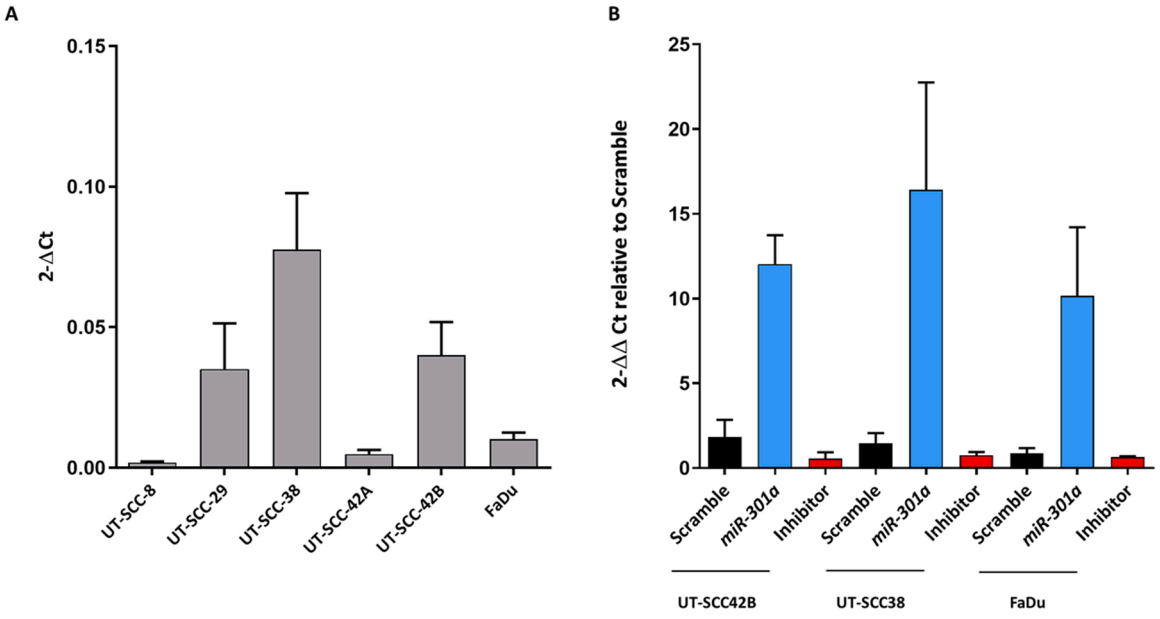


**Fig. 2.** Analysis of *miR-301a* expression in HNSCC-derived cell lines. A) *miR-301a* expression analysis in different HNSCC cell lines by qRT-PCR. Results are expressed as 2 -ΔCt. The graph represents the mean ± SD calculated from three independent experiments performed in triplicate. **B)** *miR-301a* expression in UT-SCC38, UT-SCC42B and FaDu cell lines transduced with *miR-301a* or inhibitor encoding lentiviruses by qRT-PCR. 2-ΔΔCt relative to scramble is represented. The graph represents the mean ± SD calculated from three independent experiments performed in triplicate.

doi:10.1016/j.biopha.2023.114512.

Supplementary material related to this article can be found online at doi:10.1016/j.jallcom.2022.164017.

We carried out in vivo validation using an orthotopic mouse model in which UT-SCC38 cells were sublingually inoculated. Results concordantly showed that the mitotic counts, the percentage of infiltration

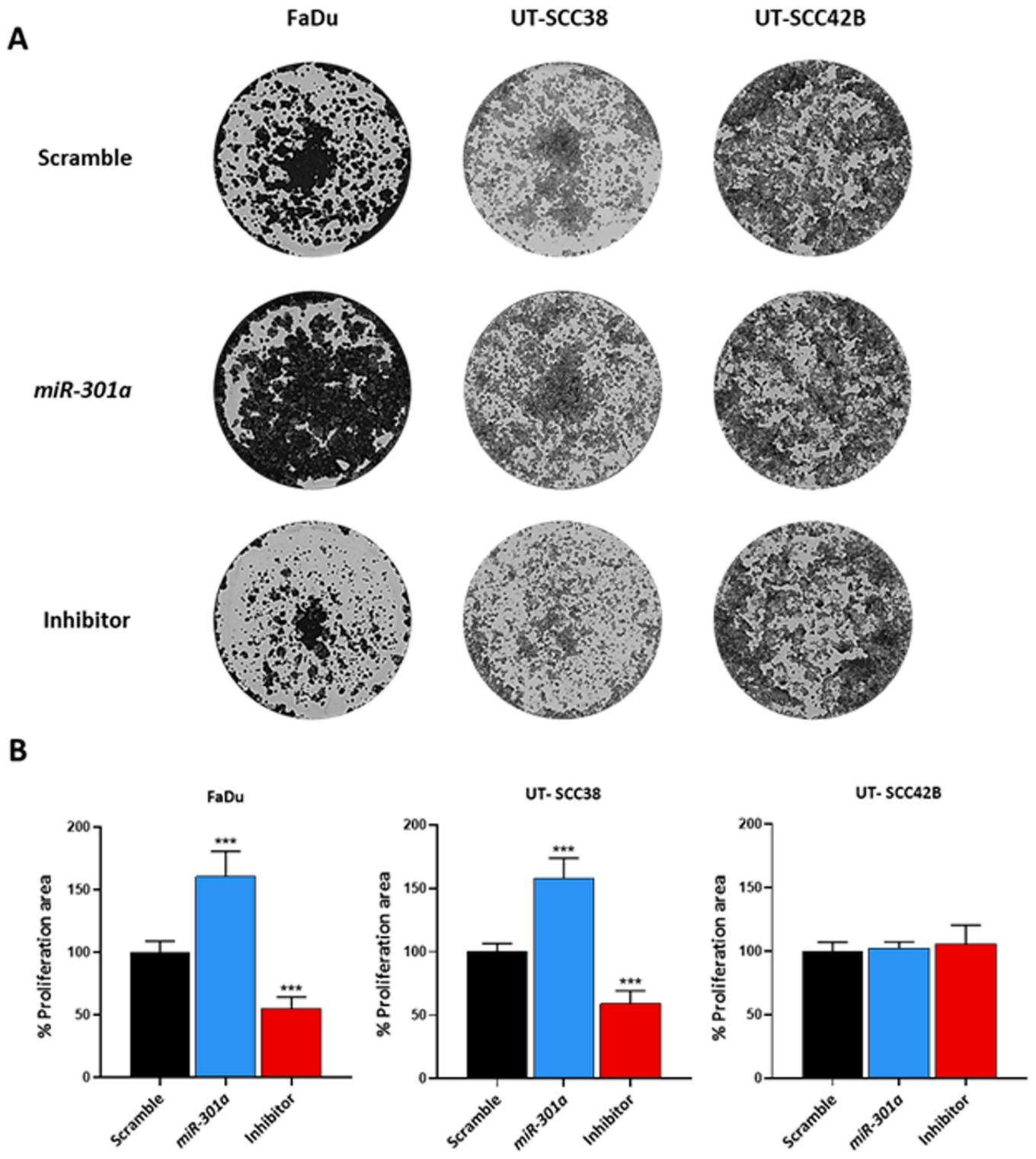


**Fig. 3.** Effect of *miR-301a* expression on colony formation in HNSCC-derived cell lines. **A**) Colony formation assays were performed in UT-SCC38, UT-SCC42B and FaDu cells transduced with either *miR-301a*, *miR-301a* inhibitor or scramble control. After 9–12 days, cells were stained with crystal violet, and **B**) Quantification of colony formation by Image J analysis software. Data were normalized to the scramble control condition and expressed as the mean ± SD of at least three independent experiments performed in triplicate * ** $p < 0.001$ by ANOVA test.

depth and the Ki67 proliferative index were significantly augmented in the subgroup of mice harboring *miR-301a*-overexpressing tumors (Fig. 5).

### 3.3. Deciphering miR-301a-mediated mechanism in HNSCC cell lines

In an attempt to elucidate the underlying mechanisms and signaling pathways involved in the oncogenic functions mediated by *miR-301a* in HNSCC, we analyzed the activation status of 37 phosphoproteins using a proteome array in the three conditions (scramble, *miR-301a* and

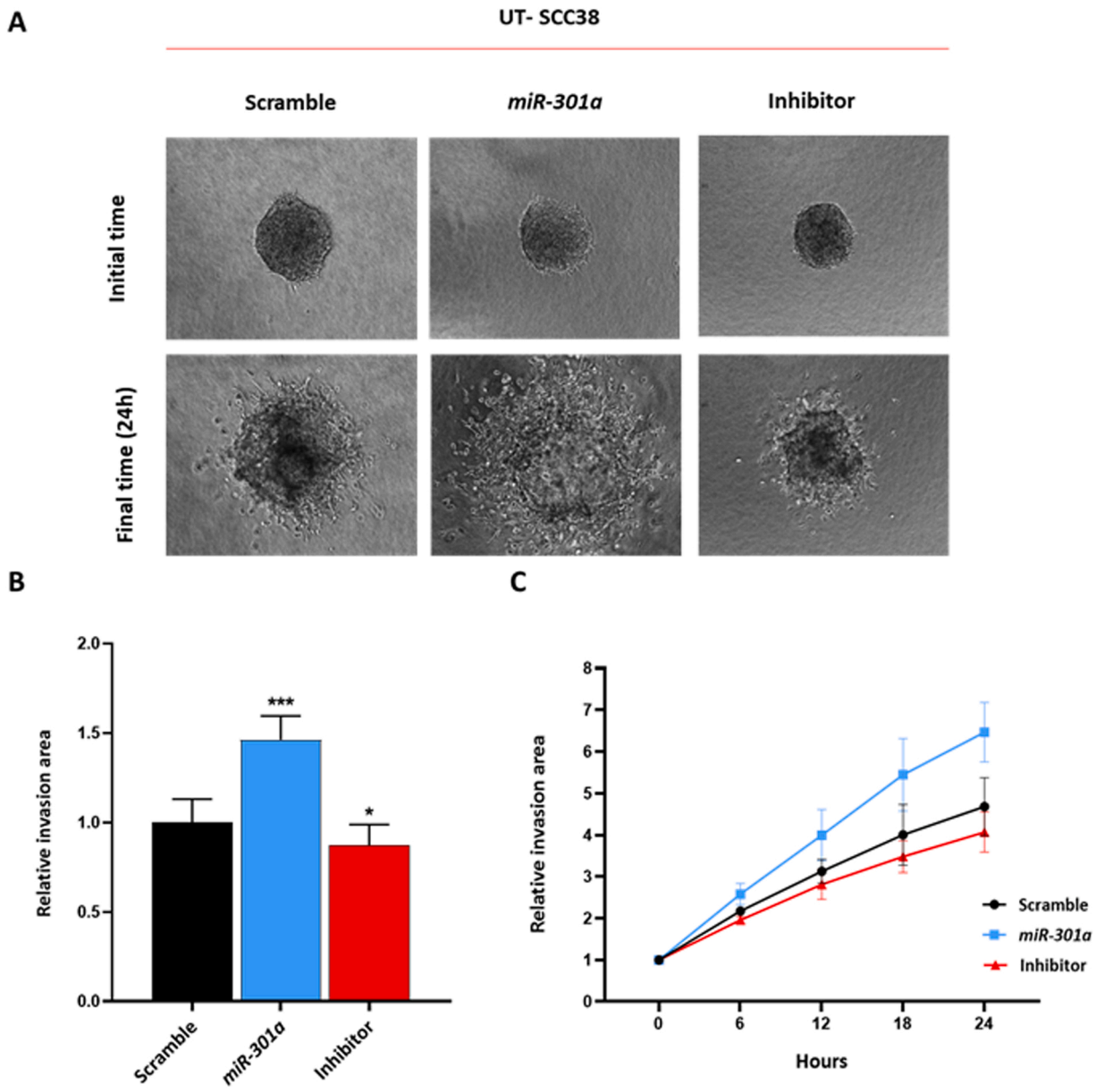


**Fig. 4.** Effect of *miR-301a* expression on 3D spheroid invasion in UT-SCC38 cells. **A)** Representative images from 3D invasion assays of collagen-embedded spheroids of UT-SCC38 cells transduced with either *miR-301a*, *miR-301a* inhibitor or scramble control at both initial and final time (24 h). **B)** Bar chart represents the relative invasive area determined by calculating the difference between the final area (t = 24 h) and the initial area (t = 0) using Image J analysis program. **C)** Relative invasive area was monitored at different time points (from 0 to 24 h). Data were normalized to scramble condition and expressed as the mean ± SD of at least three independent experiments performed in quadruplicate. * $p < 0.05$, ** $p < 0.01$ and *** $p < 0.001$ by Student t-test.

inhibitor) for the UT-SCC38 cell line. These results are summarized in a heatmap representation (Fig. 6**A**). *miR-301a* overexpression led to widespread changes in the phosphorylation levels of protein kinases, overall pointing to the PI3K and ERK pathways as major targets of this miRNA. Increased phosphorylation was observed predominantly in HSP27, MSK1/2, p70 S6 and STAT3 (Y705) kinases. Next, we performed Western blot analysis to validate some of the protein changes individually in all three HNSCC cell lines (Fig. 6**B**). As main findings, AKT (T308) phosphorylation levels were increased by *miR-301a* overexpression in both UT-SCC38 and FaDu cells (but not in UT-SCC42B), whereas p-AKT (T308) levels were reduced by *miR-301a* inhibitor (Fig. 6**B**). Notably, these changes by miRNA were specific for T308 residue, not observed in AKT (S473). Similarly, *miR-301a* inhibitor consistently reduced the phosphorylation levels of S6 (S240/244) and ERK (T202/204) in UT-SCC38 and FaDu cells, but not in UT-SCC42B cells. Besides, PTEN levels were consistently increased by *miR-301a* inhibitor in the three cell lines (Fig. 6**B**). Noteworthy, UT-SCC38 cells harboring high endogenous *miR-301a* expression exhibited higher levels of both p-AKT (T308) and p-S6 (S240/244) as compared to *miR-301a* low FaDu cells (Supplementary Fig. S4). These results are concordant to the increased levels of both activation marks p-AKT (T308) and p-S6 (S240/244) triggered by lentiviral *miR-301a* overexpression (Fig. 6B). By contrast, there were no differences between UT-SCC38 and FaDu cells in p-ERK (T202/204) activation (Supplementary Fig. S4), and consistently, p-ERK (T202/204) levels were not induced by *miR-301a* overexpression (Fig. 6B). Plausibly, this could reflect that *miR-301a* directly targets PTEN thereby modulating the activation of downstream pathway components such as p-AKT (T308) and p-S6. However, the changes in p-ERK (T202/204) only observed by *miR-301a* inhibitor may suggest an indirect effect on ERK pathway activation.

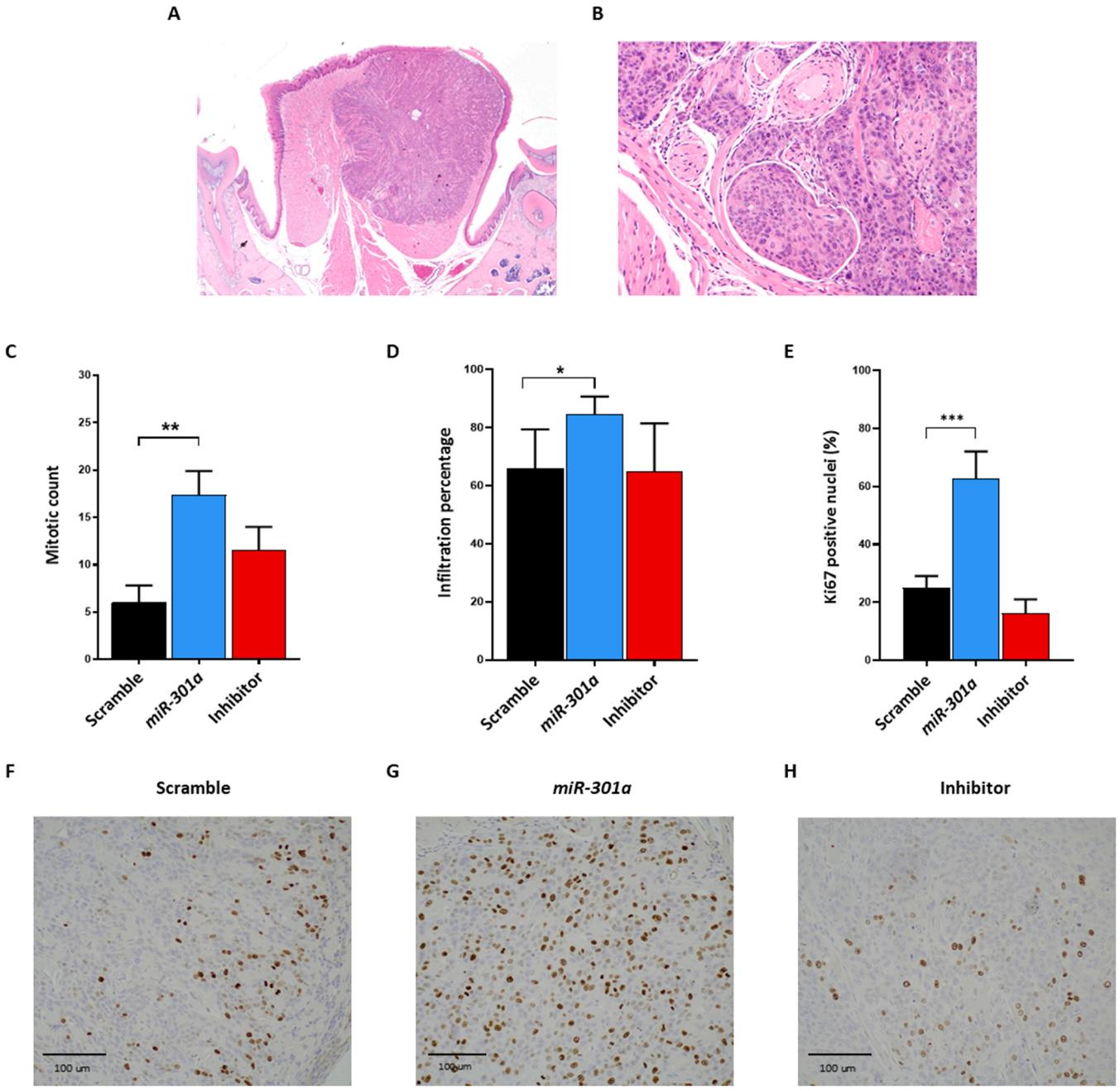


**Fig. 5.** Impact of *miR-301a* expression in an in vivo orthotopic mouse model. UT-SCC38 cells transduced with either *miR-301a*, *miR-301a* inhibitor or scramble control were sublingually inoculated in nude mice. After 17 days mice were sacrificed, tumors extracted, fixed and embedded in paraffin for histopathological evaluation. Representative HE-stained image of a tongue tumor generated in our HNSCC orthotopic model at different magnification (**A**, 1x; **B** 10x), and showing vascular invasion. The graphs represent the mitotic count **C),** the extent of tumor infiltration **D),** and Ki67-positive nuclei **E)**, as percentage. Representative images of Ki67 immunostaining for each group are shown, as indicated in **F-H** (10x magnification, scale bar 100 μm).

According to these data, PI3K/AKT/mTOR and ERK signaling pathways emerge as central nodes to mediate *miR-301a* oncogenic properties that could be potentially targeted with specific pharmacological inhibitors, as summarized in Supplementary Fig. S5.

### *3.4. PI3K and ERK inhibitors effectively abrogated the proliferative and pro-invasive effects of miR-301a in HNSCC cells*

To further confirm the implication of PI3K and ERK signaling pathways in *miR-301a*-mediated effects (i.e. cell proliferation and invasion), we selected two pharmacologic inhibitors of these pathways: BYL-719, a p110α–specific PI3K inhibitor; and PD98059, a specific MEK 1/2 inhibitor. The effect of these drugs was tested on colony formation and invasion assays. Both inhibitors were able to rescue *miR-301*-enhanced colony forming ability in UT-SCC38 and FaDu cells, but not UT-SCC42B cells (Fig. 7). Furthermore, both inhibitors completely reversed the pro-invasive effects of *miR-301a* overexpression in UT-SCC38 cells (Fig. 8). In marked contrast, UT-SCC42B was insensitive to *miR-301a* but partially sensitive to the ERK inhibitor, which is concordant with our results from colony formation assays (Supplementary Fig. S6).

## 4. Discussion

Despite advances in the treatment and management of patients with

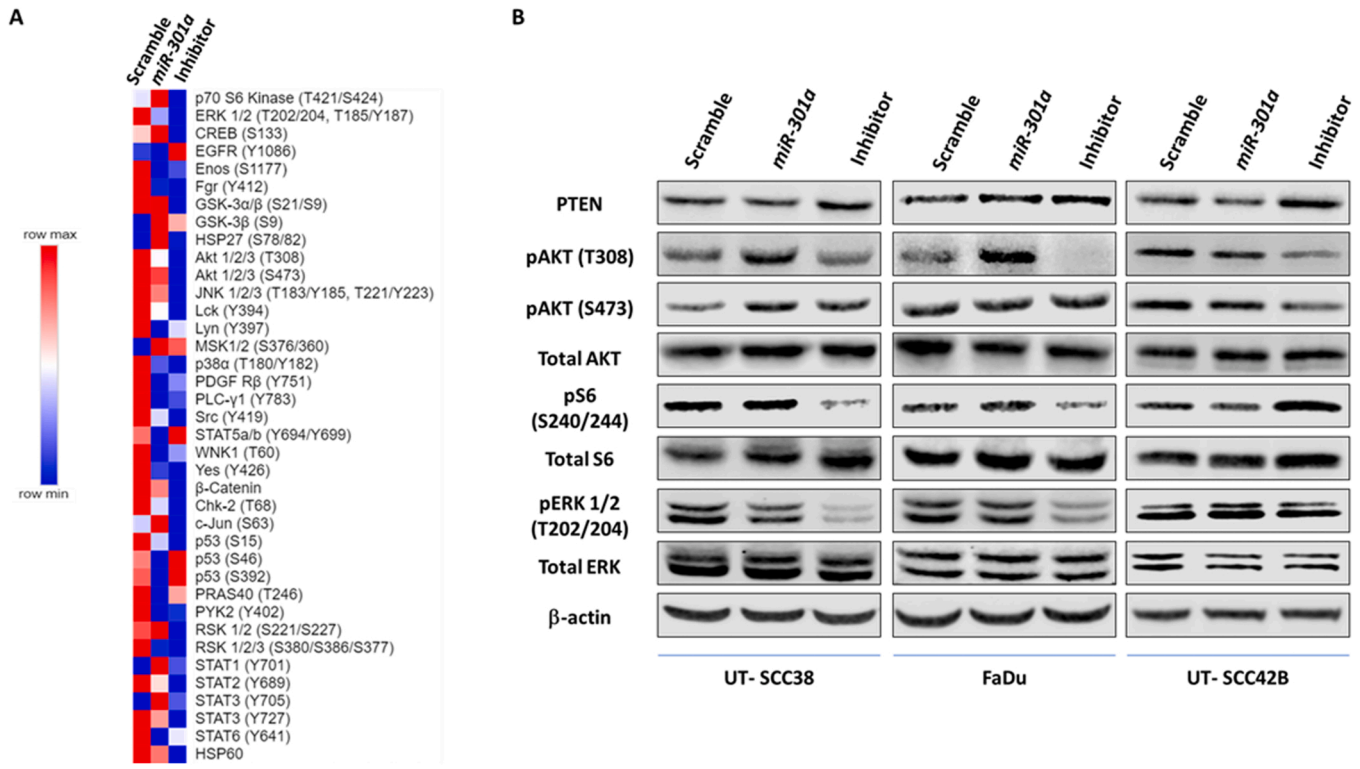


**Fig. 6.** Effect of *miR-301a* on the phosphorylation levels of cancer-related kinases. **A)** Heatmap representation using Morpheus software showing relative expression of phosphorylated proteins in UT-SCC38 cells transduced with scramble, *miR-301a* or *miR-301a* inhibitor **(B)** Western Blot validation of individual protein changes in UT-SCC38, FaDu, or UT-SCC42B cells transduced with either scramble, *miR-301a* or *miR-301a* inhibitor. These are representative images from 3 to 4 independent experiments.

HNSCC, no significant improvements of clinical outcomes have been achieved within the last decades [29]. Bioinformatic analyses revealed that miRNAs regulate more than 30% of protein-coding genes [30]. Dysregulated expression of miRNAs is frequently detected in different cancer types, which may play important roles as tumor suppressors or oncogenes [31]. Hence, these molecules have emerged as a new class of potential cancer biomarkers and therapeutic targets, which has gained attention because it offers a great opportunity for the development of novel targeted therapies for personalized medicine [32,33]. This should be particularly interesting for HNSCC, because this disease still has a high mortality and scarce treatment options.

*miR-301a*, member of oncogenic *miR-130* family, has been related to several key processes for tumor cell biology, such as invasion, migration, and cell proliferation in different cancer types [31,34–36]. However, there are limited data regarding *miR-301a* function in head and neck cancers.

The present study was aimed to investigate the possible implications of *miR-301a* dysregulation in HNSCC progression. In agreement with previous reports, *in silico* analysis of transcriptomic data from a TCGA HNSCC cohort unveiled that *miR-301a* expression levels significantly increased in primary HNSCC samples compared to patient-matched normal tissue. In depth functional and mechanistic characterization using both cellular and murine HNSCC models consistently demonstrated that *miR-301a* overexpression promoted cell proliferation and in vivo tumor growth in an orthotopic mouse model, whereas *miR-301a* inhibition decreased tumor cell growth. These results are in agreement with previous works [37,38]. Specifically, *miR-301a* overexpression in UT-SCC38 cells with the highest *miR-301a* expression, enhanced cell invasion that was diminished by *miR-301a* inhibition. Concordantly, *miR-301a*-overexpressing UT-SCC38 cells sublingually inoculated in nude mice led to tumors showing increased mitotic index and infiltration depth. These features are associated with greater tumor aggressiveness, development of metastases and appearance of recurrences, which are the principal causes of death in HNSCC [39,40]. Our results evidencing a protumorigenic role of *miR-301a* are similar to those reported for another family member *miR-130a*. The blockade of *miR-130a* with an antagomiR significantly reduced tumor growth in vivo in a xenograft OSCC model. The tumor-promoting function of *miR-130a* is mediated by *TSC1* regulation, thus leading to PI3K/Akt/mTOR pathway dysregulation [41]. In addition, it has been recently reported an oncogenic role for *miR-301a* via *SMAD4* downregulation in laryngeal squamous carcinoma. *miR-301a*-mediated downregulation of the tumor suppressor gene *SMAD4* favors tumor metastasis by modulating TGF-β/Smad signaling pathway and EMT [42].

In order to get insights into the underlying mechanisms involved in *miR-301a*-mediated oncogenic phenotypes in HNSCC, we performed a phosphoproteome array and a subsequent validation by Western blot. These findings points to PI3K/AKT/PTEN and MEK/ERK signaling pathways as crucial axes involved in mediating *miR-301a* protumoral functions. *PTEN* has been described as a target of this miRNA [34,43]. Moreover, PTEN expression was inversely correlated with *miR-301a* levels in esophageal cancer, leading to higher levels of p-AKT and BCL2 that increased the proliferation and survival of tumor cells [43]. Our results consistently demonstrated that *miR-301a* inhibitor enhanced PTEN expression in HNSCC-derived cell lines. Nevertheless, a single miRNA can regulate a wide variety of target genes and signaling pathways [44]. In fact, distinct *miR-301a* targets have been identified in different cancer types (Supplementary Table S1), including *SMAD4*, *SOCS6*, *TIMP2, MEOX2*, *VGLL4, DLC1,* and *RUNX3* [31,35,38,42,45–47].

We found several changes in PI3K/AKT/mTOR pathway components. AKT phosphorylation, specifically at T308, increased by *miR-301a* overexpression in both UT-SCC38 and FaDu cell lines, whereas it was markedly reduced by *miR-301a* inhibitor. By contrast, these changes were not observed in the phosphorylation of the serine residue S473. Moreover, S6 phosphorylation levels (S240/244) were also found to

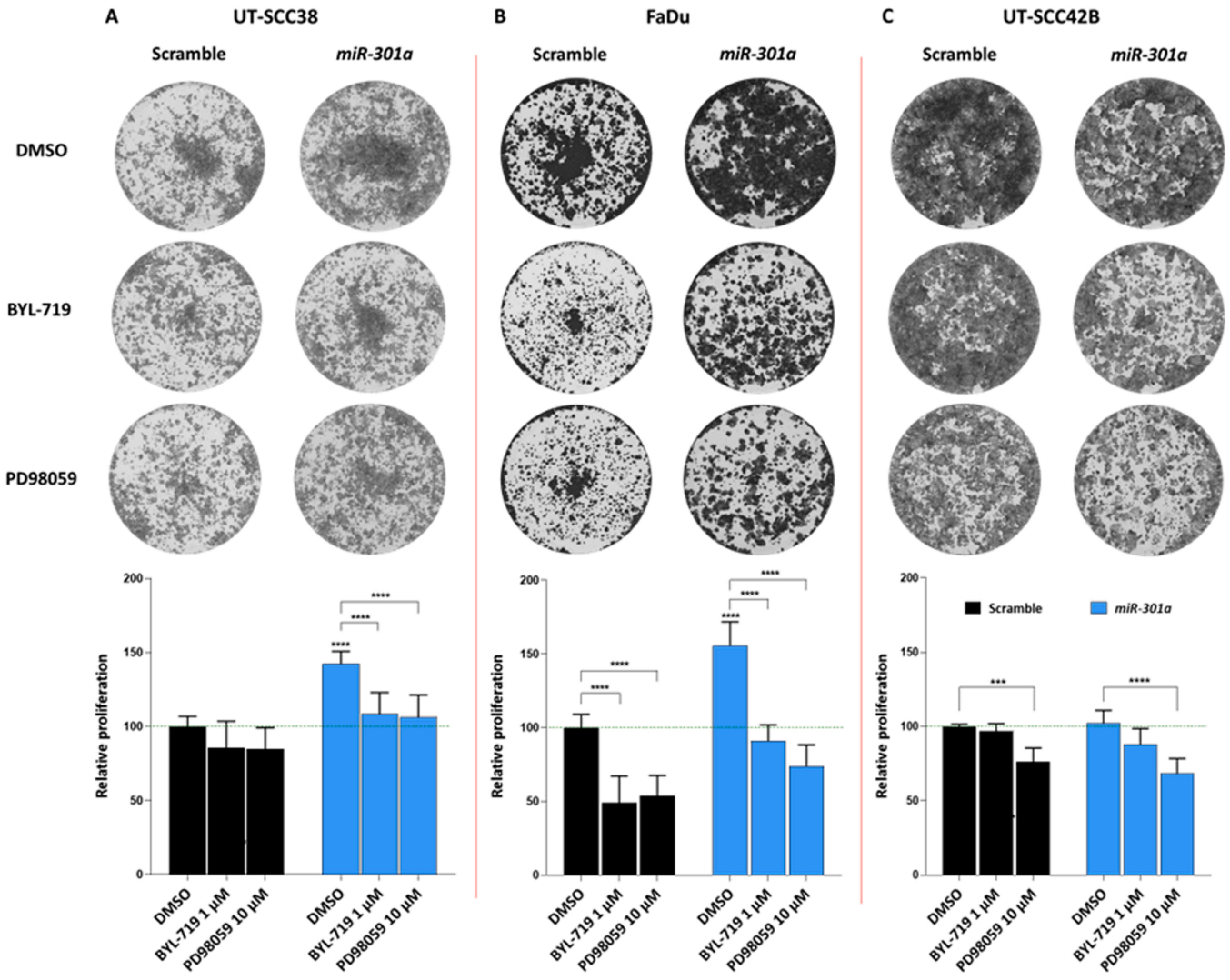


**Fig. 7.** PI3K and ERK pathway inhibitors effectively reverted the growth-promoting effects of *miR-301a* in HNSCC cell lines. Effect of PI3K inhibitor (BYL-719, 1 μM) and ERK inhibitor (PD98059, 10 μM) on colony formation was assessed on UT-SCC38 **(A)**, FaDu **(B)** and UT-SCC-42B **(C)** cell lines for 9–12 days. These are representative images from 3 to 4 independent experiments.

decrease consistently in both UT-SCC38 and FaDu cell lines by *miR-301a* inhibitor. This kinase is an important downstream effector of mTOR [48]. Previous works from our group demonstrated that PI3K/AKT/mTOR pathway is one of the most frequently and commonly dysregulated in HNSCC patients [49], by accumulating multiple genetic and molecular alterations in key components that jointly lead to pathway activation. According to our findings, *miR-301a* upregulation may be another alternative mechanism that might be contributing to PI3K/AKT/mTOR pathway activation in HNSCC, and probably other cancers. This pathway has been related to several hallmarks of cancer such as proliferation, angiogenesis, invasion, metastasis, autophagy and EMT [50]. Accordingly, it could therefore participate in the growth-promoting and pro-invasive effects observed upon *miR-301a* overexpression in our preclinical HNSCC models.

On the other hand, ERK phosphorylation (T202/204) was also found to diminish consistently by *miR-301a* inhibition in both UT-SCC38 and FaDu cells. Even though HNSCCs, in particular HPV-negative tumors, typically harbor a great diversity of mutations caused by carcinogen exposure as well as a widespread range of genomic and epigenetic alterations, most molecular changes converge into few major driver signaling pathways [51], which could be valuable to identify novel actionable cancer drivers and predictive biomarkers for targeted therapies. Among them, PI3K/AKT/mTOR pathway activated in over 70% HNSCC patients [49]. The mitogen-activated protein kinase (MAPK) signaling pathway, is also relevant and frequently altered in 5%−50% HNSCC patients. ERK2 (encoded by *MAPK1* gene) is a key component of this pathway, commonly upregulated in HNSCC [52]. Remarkably, we unprecedentedly demonstrated that pharmacologic inhibition of PI3K and ERK pathways effectively targeted the oncogenic effects of *miR-301a* overexpression in the proliferation and invasion of both UT-SCC38 and FaDu cells. By contrast, *miR-301a* overexpression had no functional effect on UT-SCC42B cells that were also insensitive to PI3K and ERK inhibitors. To our knowledge, this is the first study to report a functional link between MAPK/ERK pathway and *miR-301a*. Evidences indicate a tightly link between PI3K/AKT/mTOR pathway and other *miR-130* family members beyond *miR-301a* in HNSCC [41,53]. Since the expression levels of all oncomiR family members were found commonly upregulated in HNSCC patient samples, it is likely that pharmacologic inhibition of PI3K/AKT/mTOR could be a suitable strategy to target effectively to abrogate oncogenic *miR-130* family. Inhibition of miRNA function represents another potential therapeutic strategy. Each miRNA typically targets approximately 200 genes [54], which may enable to modulate various cancer-related signaling pathways by targeting disease-associated miRNAs.

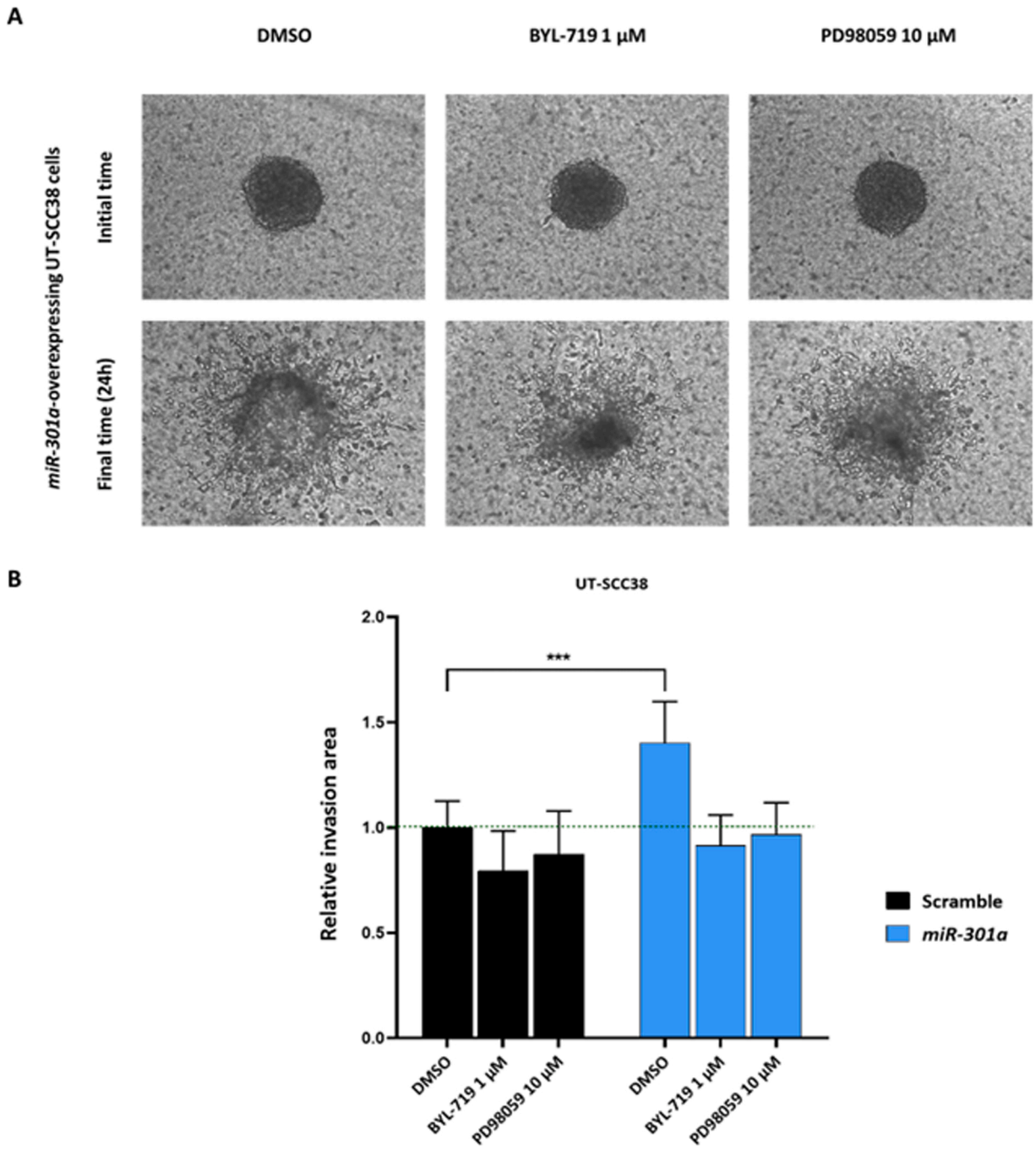


**Fig. 8.** PI3K and ERK pathway inhibitors abolished the pro-invasive effects of *miR-301a* in UT-SCC38 cells. **A)** Representative images of initial and final time (24 h) of *miR-301a*-overexpressing UT-SCC38 cells in invasion 3D assay, **B)** Relative invasive area of UT-SCC38 cell line (scramble and *miR-301a* overexpression) treated with BYL-719 1 μM and PD98059 10 μM for 24 h. Data is here represented normalized to the scramble control condition (mean ± SD of at least three independent experiments performed in triplicate). * ** $p < 0.001$ by ANOVA test.

## 5. Conclusions

Altogether our findings demonstrate that *miR-301a* upregulation is a common feature in HNSCC, which plays an oncogenic role promoting tumor growth and invasion. On this basis, *miR-301a* emerges as a candidate therapeutic target for this disease. Importantly, available PI3K and ERK inhibitors emerge as promising anti-tumor agents to effectively target *miR-301a*-mediated signal circuit hampering growth-promoting and pro-invasive functions.

## Funding

This study was supported by the Instituto de Salud Carlos III (ISCIII) through the project grants PI19/00560, PI22/00167 and CIBERONC (CB16/12/00390) and co-funded by the European Union, the Instituto de Investigación Sanitaria del Principado de Asturias (ISPA), and Fundación Bancaria Cajastur-IUOPA, Ayudas para Grupos de Investigación de Organismos del Principado de Asturias 2021–2023 (IDI/2021/000027 and IDI/2021/000079) and the FEDER Funding Program from the European Union. RGD is recipient of a Severo Ochoa predoctoral fellowship from the Principado de Asturias (BP19–063). FHP is

recipient of a Maria Zambrano grant at the University of Oviedo, and SAT recipient of a Sara Borrell postdoctoral fellowship from ISCIII (CD20/00006).

## CRediT authorship contribution statement

**Juana M. García-Pedrero, Rocío Granda-Díaz, Lorea Manterola, Saúl Álvarez-Teijeiro and Charles H. Lawrie:** development of methodology; performance of experimental procedures; acquisition, analysis, and interpretation of data. **Rocío Granda-Díaz, Lorea Manterola, Laura Santos, Vanessa García-de-la-Fuente, María Daniela Corte-Torres and María Teresa Fernández** : performance of experimental procedures. **Juana M. García-Pedrero, Rocío Granda-Díaz, Lorea Manterola, René Rodríguez, Francisco Hermida-Prado, Saúl Álvarez-Teijeiro and Juan P. Rodrigo:** analysis and interpretation of data. **Juana M. García-Pedrero, Rocío Granda-Díaz, Lorea Manterola, Juan P. Rodrigo, Saúl Álvarez-Teijeiro and Charles H. Lawrie**: conception and design, analysis and interpretation of data, manuscript writing, and financial support.

## Acknowledgments

We thank Dr. Reidar Grenman for kindly providing UT-SCC8, UT-SCC29, UT-SCC38, UT-SCC42A and UT-SCC42B, and Juan Pérez Ortega for his excellent administrative support. We want to particularly acknowledge for its collaboration the Principado de Asturias BioBank (PT17/0015/0023 and PT20/00161), financed jointly by Servicio de Salud del Principado de Asturias, Instituto de Salud Carlos III and Fundación Bancaria Cajastur and integrated in the Spanish National Biobanks Network.

### *Declarations*

#### *Ethics approval and consent to participate*

This study was performed in line with the principles of the Declaration of Helsinki. All experimental protocols were performed in accordance with the institutional guidelines of the University of Oviedo and approved by the Animal Research Ethical Committee of the University of Oviedo prior to the study (date of approval 2 September 2015; approval number PROAE46/2015).

#### *Authors' Contributions*

JMGP, RGD, LM, SAT and CL development of methodology; acquisition, analysis, and interpretation of data. RGD, LM, LS, VGF, MTF, and MDCT performance of experimental procedures. JMGP, RGD, LM, RR, FHP, SAT and JPR, analysis and interpretation of data. JMGP, RGD, JPR, LM, SAT and CL conception and design, analysis and interpretation of data, manuscript writing, and financial support. The manuscript was read and approved by all authors.

#### *Consent for publication*

All listed authors have approved the manuscript before submission, including the names and order of authors.

#### *Competing interest*

Authors declare they have no conflict of interests.

## Appendix A. Supporting information

Supplementary data associated with this article can be found in the online version at doi:10.1016/j.biopha.2023.114512.

## References

[1] H. Sung, J. Ferlay, R.L. Siegel, M. Laversanne, I. Soerjomataram, A. Jemal, F. Bray, Global Cancer Statistics 2020: GLOBOCAN Estimates of Incidence and Mortality Worldwide for 36 Cancers in 185 Countries, CA Cancer J. Clin. 71 (3) (2021) 209–249.
[2] D. Martin, M.C. Abba, A.A. Molinolo, L. Vitale-Cross, Z. Wang, M. Zaida, N.C. Delic, Y. Samuels, J.G. Lyons, J.S. Gutkind, The head and neck cancer cell oncogenome: a platform for the development of precision molecular therapies, Oncotarget 5 (19) (2014) 8906–8923.
[3] N. Denaro, M.C. Merlano, E.G. Russi, Follow-up in Head and Neck Cancer: Do More Does It Mean Do Better? A Systematic Review and Our Proposal Based on Our Experience, Clin. Exp. Otorhinolaryngol. 9 (4) (2016) 287–297.
[4] M. Acunzo, G. Romano, D. Wernicke, C.M. Croce, MicroRNA and cancer–a brief overview, Adv. Biol. Regul. 57 (2015) 1–9.
[5] M. Azar, H. Aghazadeh, H.N. Mohammed, M.R.S. Sara, A. Hosseini, N. Shomali, R. Tamjidifar, S. Tarzi, M. Mansouri, S.P. Sarand, F. Marofi, M. Akbari, H. Xu, S. S. Shotorbani, miR-193a-5p as a promising therapeutic candidate in colorectal cancer by reducing 5-FU and Oxaliplatin chemoresistance by targeting CXCR4, Int Immunopharmacol. 92 (2021), 107355.
[6] L. Zhang, Y. Liao, L. Tang, MicroRNA-34 family: a potential tumor suppressor and therapeutic candidate in cancer, J. Exp. Clin. Cancer Res 38 (1) (2019) 53.
[7] L. Adam, M. Zhong, W. Choi, W. Qi, M. Nicoloso, A. Arora, G. Calin, H. Wang, A. Siefker-Radtke, D. McConkey, M. Bar-Eli, C. Dinney, miR-200 expression regulates epithelial-to-mesenchymal transition in bladder cancer cells and reverses resistance to epidermal growth factor receptor therapy, Clin. Cancer Res 15 (16) (2009) 5060–5072.
[8] G.L. Song, M. Xiao, X.Y. Wan, J. Deng, J.D. Ling, Y.G. Tian, M. Li, J. Yin, R. Y. Zheng, Y. Tang, G.Y. Liu, MiR-130a-3p suppresses colorectal cancer growth by targeting Wnt Family Member 1 (WNT1), Bioengineered 12 (1) (2021) 8407–8418.
[9] H. Egawa, K. Jingushi, T. Hirono, Y. Ueda, K. Kitae, W. Nakata, K. Fujita, M. Uemura, N. Nonomura, K. Tsujikawa, The miR-130 family promotes cell migration and invasion in bladder cancer through FAK and Akt phosphorylation by regulating PTEN, Sci. Rep. 6 (2016) 20574.
[10] X. Xia, K. Zhang, G. Cen, T. Jiang, J. Cao, K. Huang, C. Huang, Q. Zhao, Z. Qiu, MicroRNA-301a-3p promotes pancreatic cancer progression via negative regulation of SMAD4, Oncotarget 6 (25) (2015) 21046–21063.
[11] H. Jiang, J. Lv, MicroRNA-301a-3p increases oxidative stress, inflammation and apoptosis in ox-LDL-induced HUVECs by targeting KLF7, Exp. Ther. Med 21 (6) (2021) 569.
[12] C. He, Y. Shi, R. Wu, M. Sun, L. Fang, W. Wu, C. Liu, M. Tang, Z. Li, P. Wang, Y. Cong, Z. Liu, miR-301a promotes intestinal mucosal inflammation through induction of IL-17A and TNF-alpha in IBD, Gut 65 (12) (2016) 1938–1950.
[13] L. Huang, Y. Liu, L. Wang, R. Chen, W. Ge, Z. Lin, Y. Zhang, S. Liu, Y. Shan, Q. Lin, M. Jiang, Down-regulation of miR-301a suppresses pro-inflammatory cytokines in Toll-like receptor-triggered macrophages, Immunology 140 (3) (2013) 314–322.
[14] J.Z. Zheng, Y.N. Huang, L. Yao, Y.R. Liu, S. Liu, X. Hu, Z.B. Liu, Z.M. Shao, Elevated miR-301a expression indicates a poor prognosis for breast cancer patients, Sci. Rep. 8 (1) (2018) 2225.
[15] L. Cui, Y. Li, X. Lv, J. Li, X. Wang, Z. Lei, X. Li, Expression of MicroRNA-301a and its Functional Roles in Malignant Melanoma, Cell Physiol. Biochem 40 (1–2) (2016) 230–244.
[16] Y.K. Shi, Q.L. Zang, G.X. Li, Y. Huang, S.Z. Wang, Increased expression of microRNA-301a in nonsmall-cell lung cancer and its clinical significance, J. Cancer Res Ther. 12 (2) (2016) 693–698.
[17] R.K. Nam, T. Benatar, C.J. Wallis, Y. Amemiya, W. Yang, A. Garbens, M. Naeim, C. Sherman, L. Sugar, A. Seth, MiR-301a regulates E-cadherin expression and is predictive of prostate cancer recurrence, Prostate 76 (10) (2016) 869–884.
[18] F. Ma, J. Zhang, L. Zhong, L. Wang, Y. Liu, Y. Wang, L. Peng, B. Guo, Upregulated microRNA-301a in breast cancer promotes tumor metastasis by targeting PTEN and activating Wnt/beta-catenin signaling, Gene 535 (2) (2014) 191–197.
[19] X.D. Xu, X.J. He, H.Q. Tao, W. Zhang, Y.Y. Wang, Z.Y. Ye, Z.S. Zhao, Abnormal expression of miR-301a in gastric cancer associated with progression and poor prognosis, J. Surg. Oncol. 108 (3) (2013) 197–202.
[20] W. Shi, K. Gerster, N.M. Alajez, J. Tsang, L. Waldron, M. Pintilie, A.B. Hui, J. Sykes, C. P'ng, N. Miller, D. McCready, A. Fyles, F.F. Liu, MicroRNA-301 mediates proliferation and invasion in human breast cancer, Cancer Res 71 (8) (2011) 2926–2937.
[21] X. Li, M. Zhong, J. Wang, L. Wang, Z. Lin, Z. Cao, Z. Huang, F. Zhang, Y. Li, M. Liu, X. Ma, miR-301a promotes lung tumorigenesis by suppressing Runx3, Mol. Cancer 18 (1) (2019) 99.
[22] C.J. Lin, J.R. Grandis, T.E. Carey, S.M. Gollin, T.L. Whiteside, W.M. Koch, R. L. Ferris, S.Y. Lai, Head and neck squamous cell carcinoma cell lines: established models and rationale for selection, Head. Neck 29 (2) (2007) 163–188.
[23] J.B. Poell, R.J. van Haastert, T. de Gunst, I.J. Schultz, W.M. Gommans, M. Verheul, F. Cerisoli, A. van Puijenbroek, P.I. van Noort, G.P. Prevost, R.Q. Schaapveld, E. Cuppen, A functional screen identifies specific microRNAs capable of inhibiting human melanoma cell viability, PLoS One 7 (8) (2012), e43569.
[24] J.B. Poell, R.J. van Haastert, F. Cerisoli, A.S. Bolijn, L.M. Timmer, B. Diosdado-Calvo, G.A. Meijer, A.A. van Puijenbroek, E. Berezikov, R.Q. Schaapveld, E. Cuppen, Functional microRNA screening using a comprehensive lentiviral human microRNA expression library, BMC Genom. 12 (2011) 546.
[25] C.H. Lawrie, N.J. Saunders, S. Soneji, S. Palazzo, H.M. Dunlop, C.D. Cooper, P. J. Brown, X. Troussard, H. Mossafa, T. Enver, F. Pezzella, J. Boultwood, J. S. Wainscoat, C.S. Hatton, MicroRNA expression in lymphocyte development and malignancy, Leukemia 22 (7) (2008) 1440–1446.

[26] M.A. Villaronga, F. Hermida-Prado, R. Granda-Diaz, S.T. Menendez, S. Alvarez-Teijeiro, M. Quer, I. Vilaseca, E. Allonca, M. Garzon-Arango, V. Sanz-Moreno, A. Astudillo, J.P. Rodrigo, J.M. Garcia-Pedrero, Immunohistochemical Expression of Cortactin and Focal Adhesion Kinase Predicts Recurrence Risk and Laryngeal Cancer Risk Beyond Histologic Grading, Cancer Epidemiol. Biomark. Prev. 27 (7) (2018) 805–813.
[27] D.S. Chandrashekar, B. Bashel, S.A.H. Balasubramanya, C.J. Creighton, I. Ponce-Rodriguez, B. Chakravarthi, S. Varambally, UALCAN: A Portal for Facilitating Tumor Subgroup Gene Expression and Survival Analyses, Neoplasia 19 (8) (2017) 649–658.
[28] N. Cancer Genome Atlas, Comprehensive genomic characterization of head and neck squamous cell carcinomas, Nature 517 (7536) (2015) 576–582.
[29] D.E. Johnson, B. Burtness, C.R. Leemans, V.W.Y. Lui, J.E. Bauman, J.R. Grandis, Head and neck squamous cell carcinoma, Nat. Rev. Dis. Prim. 6 (1) (2020) 92.
[30] M. Li, C. Marin-Muller, U. Bharadwaj, K.H. Chow, Q. Yao, C. Chen, MicroRNAs: control and loss of control in human physiology and disease, World J. Surg. 33 (4) (2009) 667–684.
[31] Y. Fang, B. Sun, J. Xiang, Z. Chen, MiR-301a promotes colorectal cancer cell growth and invasion by directly targeting SOCS6, Cell Physiol. Biochem 35 (1) (2015) 227–236.
[32] J. Carron, C. Torricelli, J.K. Silva, G.S.R. Queiroz, M.M. Ortega, C.S.P. Lima, G. J. Lourenco, microRNAs deregulation in head and neck squamous cell carcinoma, Head. Neck 43 (2) (2021) 645–667.
[33] A. Min, C. Zhu, S. Peng, S. Rajthala, D.E. Costea, D. Sapkota, MicroRNAs as Important Players and Biomarkers in Oral Carcinogenesis, Biomed. Res Int (2015) (2015), 186904.
[34] J. Li, D. Jiang, Q. Zhang, S. Peng, G. Liao, X. Yang, J. Tang, H. Xiong, J. Pang, MiR-301a Promotes Cell Proliferation by Repressing PTEN in Renal Cell Carcinoma, Cancer Manag Res 12 (2020) 4309–4320.
[35] B. Liang, J.J. Yin, X.R. Zhan, MiR-301a promotes cell proliferation by directly targeting TIMP2 in multiple myeloma, Int J. Clin. Exp. Pathol. 8 (8) (2015) 9168–9174.
[36] W. Zhang, T. Zhang, R. Jin, H. Zhao, J. Hu, B. Feng, L. Zang, M. Zheng, M. Wang, MicroRNA-301a promotes migration and invasion by targeting TGFBR2 in human colorectal cancer, J. Exp. Clin. Cancer Res 33 (1) (2014) 113.
[37] M. Kawano, K. Tanaka, I. Itonaga, T. Iwasaki, H. Tsumura, MicroRNA-301a promotes cell proliferation via PTEN targeting in Ewing's sarcoma cells, Int J. Oncol. 48 (4) (2016) 1531–1540.
[38] M. Wang, C. Li, B. Yu, L. Su, J. Li, J. Ju, Y. Yu, Q. Gu, Z. Zhu, B. Liu, Overexpressed miR-301a promotes cell proliferation and invasion by targeting RUNX3 in gastric cancer, J. Gastroenterol. 48 (9) (2013) 1023–1033.
[39] F. Duprez, D. Berwouts, W. De Neve, K. Bonte, T. Boterberg, P. Deron, W. Huvenne, S. Rottey, M. Mareel, Distant metastases in head and neck cancer, Head. Neck 39 (9) (2017) 1733–1743.
[40] S. Colella, K.L. Richards, L.L. Bachinski, K.A. Baggerly, S. Tsavachidis, J.C. Lang, D. E. Schuller, R. Krahe, Molecular signatures of metastasis in head and neck cancer, Head. Neck 30 (10) (2008) 1273–1283.
[41] K. Mallela, S. Shivananda, K.S. Gopinath, A. Kumar, Oncogenic role of MiR-130a in oral squamous cell carcinoma, Sci. Rep. 11 (1) (2021) 7787.
[42] Y. Lu, W. Gao, C. Zhang, S. Wen, H. Huangfu, J. Kang, B. Wang, Hsa-miR-301a-3p Acts as an Oncogene in Laryngeal Squamous Cell Carcinoma via Target Regulation of Smad4, J. Cancer 6 (12) (2015) 1260–1275.
[43] N. Zhang, J.F. Liu, MicroRNA (MiR)-301a-3p regulates the proliferation of esophageal squamous cells via targeting PTEN, Bioengineered 11 (1) (2020) 972–983.
[44] L.P. Lim, N.C. Lau, P. Garrett-Engele, A. Grimson, J.M. Schelter, J. Castle, D. P. Bartel, P.S. Linsley, J.M. Johnson, Microarray analysis shows that some microRNAs downregulate large numbers of target mRNAs, Nature 433 (7027) (2005) 769–773.
[45] H. Liu, G. Wang, MicroRNA-301a-3p promotes triple-negative breast cancer progression through downregulating MEOX2, Exp. Ther. Med 22 (3) (2021) 945.
[46] J. Hu, J. Ruan, X. Liu, C. Xiao, J. Xiong, MicroRNA-301a-3p suppressed the progression of hepatocellular carcinoma via targeting VGLL4, Pathol. Res Pr. 214 (12) (2018) 2039–2045.
[47] Z. Wu, Y. Li, G. Zhang, Downregulation of microRNA-301a inhibited proliferation, migration and invasion of non-small cell lung cancer by directly targeting DLC1, Oncol. Lett. 14 (5) (2017) 6017–6023.
[48] B.F. Bahrami, P. Ataie-Kachoie, M.H. Pourgholami, D.L. Morris, p70 Ribosomal protein S6 kinase (Rps6kb1): an update, J. Clin. Pathol. 67 (12) (2014) 1019–1025.
[49] D. Garcia-Carracedo, M.A. Villaronga, S. Alvarez-Teijeiro, F. Hermida-Prado, I. Santamaria, E. Allonca, L. Suarez-Fernandez, M.V. Gonzalez, M. Balbin, A. Astudillo, P. Martinez-Camblor, G.H. Su, J.P. Rodrigo, J.M. Garcia-Pedrero, Impact of PI3K/AKT/mTOR pathway activation on the prognosis of patients with head and neck squamous cell carcinomas, Oncotarget 7 (20) (2016) 29780–29793.
[50] C. Harsha, K. Banik, H.L. Ang, S. Girisa, R. Vikkurthi, D. Parama, V. Rana, B. Shabnam, E. Khatoon, A.P. Kumar, A.B. Kunnumakkara, Targeting AKT/mTOR in Oral Cancer: Mechanisms and Advances in Clinical Trials, Int J. Mol. Sci. 21 (9) (2020).
[51] R. Iglesias-Bartolome, D. Martin, J.S. Gutkind, Exploiting the head and neck cancer oncogenome: widespread PI3K-mTOR pathway alterations and novel molecular targets, Cancer Disco 3 (7) (2013) 722–725.
[52] M. Prasad, J. Zorea, S. Jagadeeshan, A.B. Shnerb, S. Mathukkada, J. Bouaoud, L. Michon, O. Novoplansky, M. Badarni, L. Cohen, K.M. Yegodayev, S. Tzadok, B. Rotblat, L. Brezina, A. Mock, A. Karabajakian, J. Fayette, I. Cohen, T. Cooks, I. Allon, O. Dimitstein, B. Joshua, D. Kong, E. Voronov, M. Scaltriti, Y. Carmi, C. Conde-Lopez, J. Hess, I. Kurth, L.G.T. Morris, P. Saintigny, M. Elkabets, MEK1/2 inhibition transiently alters the tumor immune microenvironment to enhance immunotherapy efficacy against head and neck cancer, J. Immunother. Cancer 10 (3) (2022).
[53] H. Li, P. Liu, D. Li, Z. Wang, Z. Ding, M. Zhou, X. Chen, M. Miao, J. Ding, W. Lin, Y. Liu, X. Zha, STAT3/miR-130b-3p/MBNL1 feedback loop regulated by mTORC1 signaling promotes angiogenesis and tumor growth, J. Exp. Clin. Cancer Res 41 (1) (2022) 297.
[54] A. Esquela-Kerscher, F.J. Slack, Oncomirs - microRNAs with a role in cancer, Nat. Rev. Cancer 6 (4) (2006) 259–269.